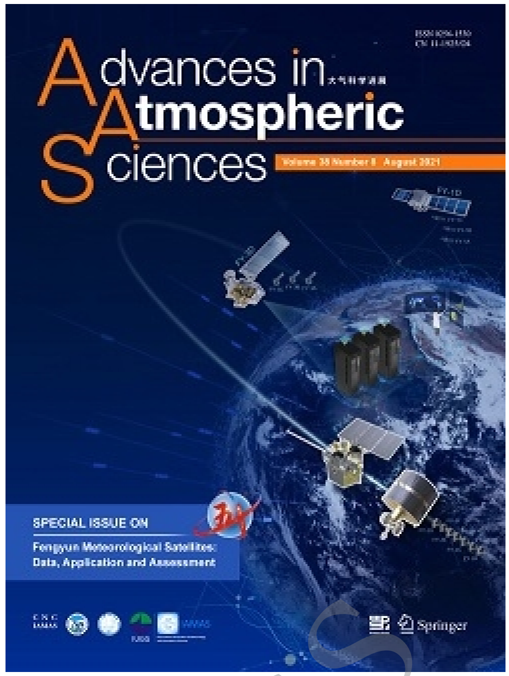

Evaluation of long-term performance of microwave radiometers onboard Chinese Fengyun satellites

Journal:	*Advances in Atmospheric Sciences*
Manuscript ID	AAS-2022-0199.R3
Manuscript Type:	Original Article
Date Submitted by the Author:	04-Jan-2023
Complete List of Authors:	He, Wenying Chen, Hongbin; Institue of Atmospheric Physics, Chinese Academy of Sciences, LAGEO XIA, Xiang-Ao; Institute of Atmospheric Physics, Chinese Academy of Sciences, Laboratory for Middle Atmosphere and Global Environment Observation (LAGEO) Wu, Shengli; National Satellite Meteorological Center of China Meteorological Administration Zhang, Peng; China Meteorological Administration National Satellite Meteorological Center,

Evaluation of the long-term performance of microwave radiometers onboard Chinese Fengyun satellites

Wenying HE *[1], Hongbin CHEN[1], Xiangao XIA[1], Shengli WU[2], Peng ZHANG[2]

[1]LAGEO, Institute of Atmospheric Physics, Chinese Academy of Sciences, Beijing, China, 100029

[2]National Satellite Meteorological Center, China Meteorological Administration, Beijing 100081, China

ABSTRACT

Accurate brightness temperature (BT) is a top priority for retrievals of atmospheric and surface properties. Microwave Radiation Imagers (MWRI) on Chinese Fengyun-3 (FY-3) serial polar-orbiting satellites have been providing abundant BT data since 2008, showing great potential for retrievals of atmospheric parameters and surface properties. Much work has been done to evaluate short-term MWRI observations, but it remains unclear on the long-term performance of MWRI. In this paper, the operational MWRI BT during 2012-2019 was carefully examined by using the simultaneous Advanced Microwave Scanning Radiometer 2 (AMSR2) BTs as the reference. A significant correlation between BTs from MWRI and AMSR2 was found. The BT difference between MWRI/FY3B and AMSR2 during 2012-2019 increased gradually over time. As compared with MWRI/FY3B, MWRI/FY3D BTs over land were much closer to those of AMSR2. The ascending and descending orbit difference for MWRI/FY3D is also much smaller than that for MWRI/FY3B. Both suggest the improvement of MWRI/FY3D over MWRI/FY3B. A substantial BT difference between AMSR2 and MWRI was found over water, even exceeding 5 K at the vertical polarization channels. A similar BT difference was found over polar water based on the simultaneous conical overpassing (SCO) method. Radiative transfer model simulations suggested the substantial BT differences at the vertical polarization

*Corresponding author : Wenying HE
Email: hwy@mail.iap.ac.cn

channels of MWRI and AMSR2 over water were partly accounted for by their difference in the incident angle; however, the underestimation of the operational MWRI BT over the water was still a very important issue. The preliminary assessment of the operational and recalibrated MWRI BT demonstrated that MWRI BTs at the vertical polarization channels were substantially improved after the recalibration, especially the obvious underestimation of the operational MWRI BT at 10V and 37V over water was corrected, and the recalibration also reduces the time-dependent biases.

Keywords: FY-3 satellites, MWRI, AMSR2, Brightness temperature, recalibration
https://doi.org/10.1007/s00376-023-2199-2

Article Highlights:

- The operational MWRI BT measurements were significantly correlated with those of AMSR2 and the BT difference between MWRI/FY3B and AMSR2 during 2012-2019 increased gradually over time.
- MWRI/FY3D BT over land was much closer to that of AMSR2 relative to MWRI/FY3B; however, a substantial BT difference between AMSR2 and MWRI was found over water.
- The substantial BT differences at the vertical polarization channels over water were partly attributed to the different incident angles between MWRI and AMER2; however, the underestimation of MWRI BT over the water was still a very important issue.
- MWRI BTs were substantially improved after the recalibration, more specifically, the obvious underestimation of the operational MWRI BT at 10V and 37V over the water was corrected.

1. Introduction

FY-3 series of China polar-orbiting meteorological satellites have been launched in succession from 2008-2021 (Dong et al., 2009; Yang et al., 2011; Lu et al., 2016; Zhang et al., 2019, 2022), including FY-3A (May 2008), FY-3B (Nov. 2010), FY-3C (Sep. 2013), FY-3D (Nov. 2017) and FY-3E (Jul. 2021). Microwave Radiation Imager (MWRI) is one of the primary sensors on FY-3 satellites. MWRI is a conical-scanning microwave imager with frequencies varying from 10.65 GHz to 89 GHz, which are sensitive to the surface, column water vapor, cloud, and precipitation (Tang and Zou, 2017; Li et al., 2022). MWRI observations have been used to study tropical cyclones and soil moisture (Zhang et al., 2015; Cui et al., 2016; Sun et al., 2016; Xian et al., 2021).

To guarantee and check high-quality MWRI measurements, many calibrations and validations have been performed since 2008. The calibration and correction procedures for MWRI on FY-3A/B were performed, in which the linearity and non-linearity corrections were carefully considered (Yang et al., 2011). Liu et al. (2014) introduced an antenna surface calibration system for MWRI/FY3C. Given the fact that nonlinear variation was an essential factor impacting the calibration accuracy, the nonlinear characteristics of MWRI/FY3D were investigated and an optimal calculation method was proposed (Chen et al., 2019; Dong et al., 2020). Short-term MWRI/FY3B BTs in 2010 were compared with the observations from the Aqua Advanced Microwave Scanning Radiometer (AMSR-E) and radiative transfer model (RTM) simulations, showing a small bias of MWRI (Yang et al., 2012). MWRI/FY3B BTs in the early six months after launching were carefully checked. On-orbit MWRI BTs were stable, with a maximum fluctuation of the coldest reference values at all channels no more than 1.8 K (Qiao et al., 2012). The geolocation errors of MWRI on FY3B/3C were analyzed and corrected (Tang et al.,2016; Liu et al., 2021). The quality of MWRI/FY3C was evaluated by comparison with RTM results, showing a 1-2 K difference between ascending and descending orbits (Lawrence et al., 2017; Zeng and Jiang, 2021). Zhang et al. (2019) compared the parameters of the calibration equation for MWRI/FY3C and found the high value of the hot load reflector was the main cause of the bias, which was corrected, and thereby the bias between ascending and descending orbits was reduced.

These previous studies were primarily based on short-term observations after lunching of MWRI. Since there are long-term records from MWRI on FY-3 serial satellites, it is highly critical to assess the long-term quality of MWRI data, which is a top priority for the retrievals of atmospheric and surface properties. Given the fact that the MWRI channels are nearly identical to that of the Advanced Microwave Scanning Radiometer-2 (AMSR2) instrument on the GCOM-W1 satellite (Takashi et al., 2015), the inter-comparison between MWRI and AMSR2 observations from 2012 to 2019 was investigated, which is, as far as we know, the first attempt to evaluate the long-term performance of MWRI by using the advanced AMSR2 measurements. Furthermore, we also used RTM simulations to discuss the causes for the bias between MWRI and AMSR2 measurements, which would shed new light on how to improve MWRI measurements in near future.

2. Instruments and data

Both MWRI and AMSR2 are conical-scanning microwave imagers (Table 1), with nearly identical central frequencies from 10.65 GHz to 89 GHz. Due to very short-term MWRI observations from FY-3A and the larger Equator Crossing Time (ETC) gap between FY3C and GCOM-W1, the inter-comparison here was mainly focused on FY3B and FY3D satellites.

Table 1 Satellites and angles for MWRI and AMSR2

	MWRI			AMSR2
Satellite	FY3B	FY3C	FY3D	GCOM-W1
Launched	Nov. 2010	Sep. 2013	Nov. 2017	May 2012
Equator Crossing Time	13:38 Ascending	10:15 Descending	14:00 Ascending	13:30 Ascending
Incident angle	53.1°			55°

The real-time, operational MWRI L1B radiance data on FY-3B/3D are available online (http://satellite.cma.gov.cn/PortalSite/Data/Satellite.aspx), including the calibrated BT and land cover at scanning pixels. The land cover is from the international geosphere biosphere program (IGBP) classification system. The operational L1B radiance data of MWRI were directly compared against the Global Precipitation Measurement (GPM) L1C AMSR2 Product. The latter is transformed from the equivalent AMSR2/GCOM-W1 L1B radiance data using GPM Microwave Imager (GMI) as the reference standard. As successor of Aqua/AMSR-E (launched in May 2002), AMSR2 was improved on-board calibration target, resulting in reduction of annual TB variation and improvement of TB stability, for instance, AMSR2 L1B brightness temperature precision or random error +/-0.3K, accuracy within +/-1.5K(Ebuchi1 et al., 2021). After the GPM core satellite was launched in Feb. 2014, GMI was used as a calibration standard to inter-calibrate different imagers aboard other polar-orbiting satellites (Skofronick-Jackson et al., 2017). The GPM Intersatellite Calibration Working Group found AMSR2 L1B existing a substantial cold-scene warm calibration bias with respect to GMI (Berg et al., 2016), then established the calibration adjustment to generate GPM L1C AMSR2 data. Considering GMI BT with high accuracy levels for all channels within 0.4 K and stability within 0.2 K (Wentz and Draper, 2016), the quality of GPM L1C AMSR2 should be better than the original AMSR2/GCOM-W1 L1B radiance. Hence GPM L1C AMSR2 radiance data is the optimal choice for comparing with MWRI, which makes it possible for MWRI to be tractable to the international reference.

MWRI and AMSR2 BT data during July 1-5, 2012-2019 between 70°E-135°E and 20°N-50°N were compared. Hence, there are eight years of matching data for MWRI/FY3B (2012-2019) and two years of matching data for MWRI/FY3D (2018-2019). The BT observations were matched if the temporal/spatial difference between MWRI and AMSR2 observations is less than 15 minute/5 km. To mitigate uncertainties due to inhomogeneous atmosphere or land surface, an extra constraint was used in the matching process, i.e., the standard deviations of BT should be no more than 2 K in the area around the matched samples.

3. Results

3.1. BT comparison for MWRI and AMSR2 over land and water

The BT differences at the 8 channels from 10.65 GHz to 37.0 GHz (in both vertical and horizontal polarization channels, denoted as 10V, 10H, 19V, 19H, 23V, 23H, 37V, and 37H, respectively) were mainly analyzed in this work. To see the BT difference clearly, the matching pairs were divided into two subgroups, i.e., over water and land based on their land cover information. First, both BT at the 8 channels shows a good linear correlation (R varies from 0.94 to 1.0), especially high agreement of MWRI with AMSR2 at 19V onboard either FY3B or FY3D. A small standard deviation (STD) of BT difference (varying from 0.8 to 1.3 K) occurs at the vertical polarization channels of MWRI on both FY3B and FY3D. Second, the agreement of AMSR2 and MWRI/FY3D appears better than that onboard FY3B, which is reflected in the obvious reduction on the mean bias error (MBE) from 2-4 K on FY3B to 0-2 K on FY3D. The STD of MWRI/FY3D is also smaller than that of MWRI/FY3B, particularly at the horizontal polarization channels.

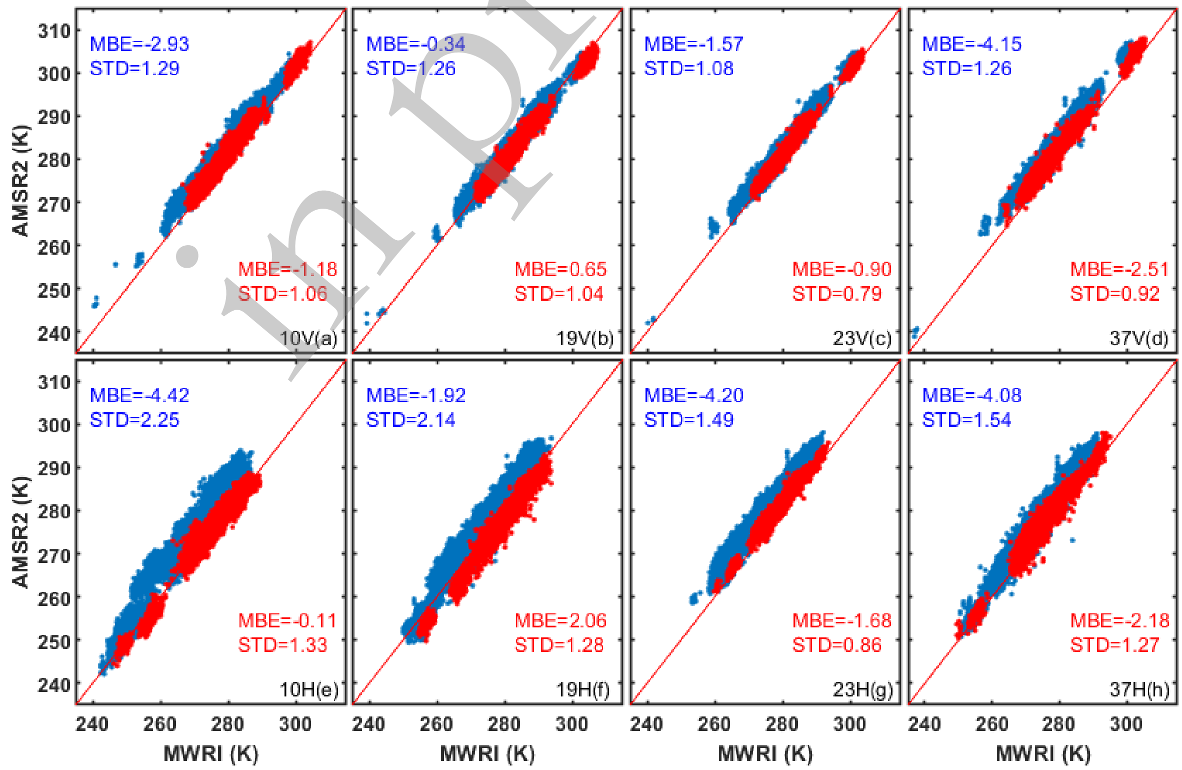

Fig.1 Scatter plots of matched BT at 8 channels for AMSR2-MWRI/ FY3B during 2012-2019 (blue) and AMSR2-MWRI/FY3D during 2018-2019 (red) over land. The corresponding statistics parameters are shown in the same color.

The matched pairs over water are shown in Fig.2. It is seen that most MWRI BTs are smaller than AMSR2 measurements, especially the MBE at the vertically polarized channels exceeding 5 K, even up to 10 K at 10V and 37V. This is almost 3 times larger than that at the corresponding horizontally polarized channels. In addition, the MBE at 23H (~8K) is larger than that at the other three horizontal channels (2-3 K).

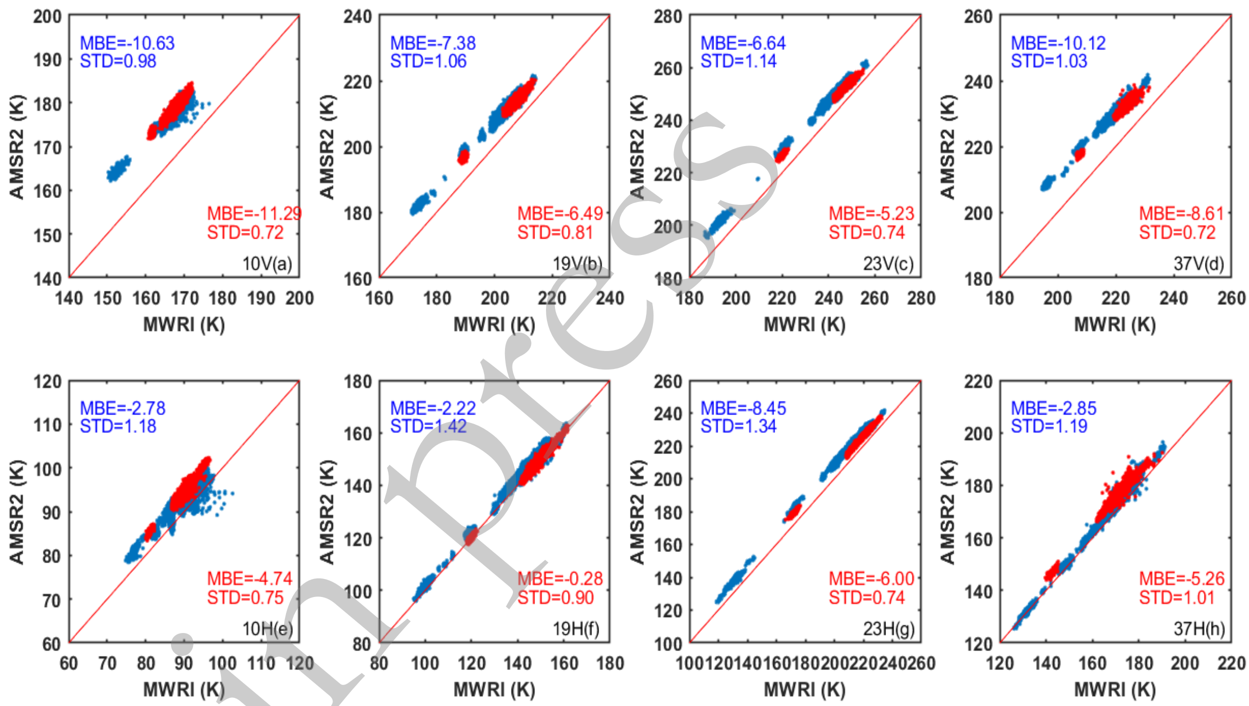

Fig.2 Same as Fig.1 except for the water group.

From the BT difference shown in Fig.1 and Fig.2, there are two interesting points that merit further mention. First, the majority of MWRI BTs are smaller than AMSR2 measurements, no matter whether it is onboard FY3B or on FY3D. Second, we can also see a clear improvement in the performance of MWRI onboard the FY3D as compared with that on FY3B, which is supported by the fact that the BT difference between FY3D and AMSR2 over land is mostly less than 2 K; however, it is up to 2-4 K regarding FY3B. The improvement in MWRI onboard FY3D is much more outstanding at the horizontal polarization channels than that at the vertical channels. It is implied that relatively high-quality MWRI observations on FY3D would be beneficial for the correction of BT measurements of MWRI on FY3B, thereby maintaining consistency in the long-term MWRI data.

To evaluate the long-term performance of MWRI BT data onboard FY3B, the annual BT difference between AMSR2 and MWRI/ FY3B during 2012-2019 is shown in Fig.3. The boxplot of BT difference over land (filled) and water (unfilled) groups are clearly separated at the vertical polarization channels but they are close to each other at the horizontal polarization channels. Overland, the annual median BT differences (July 1-5 each year, hereinafter) at both the horizontal and vertical polarizations channels increase in absolute magnitude over time. Overwater, it is still clear that the BT difference at the vertical polarization channels is quite larger than that at corresponding horizontal channels, especially at 10V and 37V the median BT difference exceeds 10 K. The annual BT differences at both polarization channels over water increase slightly during 2012-2019. The gradually increase in absolute magnitude of annual BT difference in eight years indicate the gradually increasing measurement uncertainty of operational calibrated MWRI on FY3B during 2012-2019.

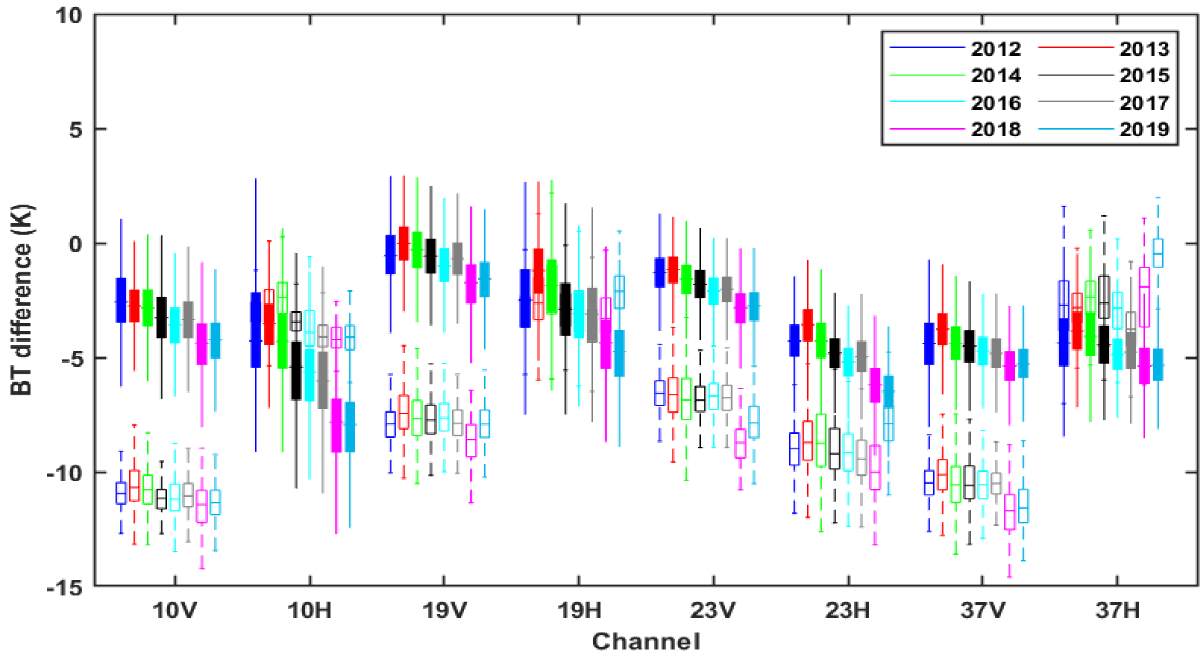

Fig.3 The boxplot of annual BT difference between MWRI/FY3B and AMSR2 during 2012-2019 over land (filled) and water (unfilled).

For AMSR2-MWRI/FY3D matching pairs in 2018-2019, the variations of BT difference in each year are small and close (not shown), which implies the stability of MWRI on FY3D in the two years.

3.2. Ascending and descending difference

The obvious difference between ascending and descending orbits for MWRI/FY3C was found by Lawrence et al. (2017), which was likely due to different errors in the hot load. The question that arises here is that dose this happened to MWRI on FY3B/3D? We group the matching MWRI- AMSR2 samples in 2012-2019 for FY3B and 2018-2019 for FY3D based on MWRI ascending (A) and descending (D) orbits. Fig.4 shows the MBE of MWRI-AMSR2 BT difference for both A and D orbits over land and water. The BT difference for the descending orbit of MWRI/FY3B is generally smaller than that for the ascending one no matter over land or water surface. This phenomenon did not occur for MWRI/FY3D, reflecting the improvement of MWRI/FY3D in reducing the difference between ascending and descending orbits.

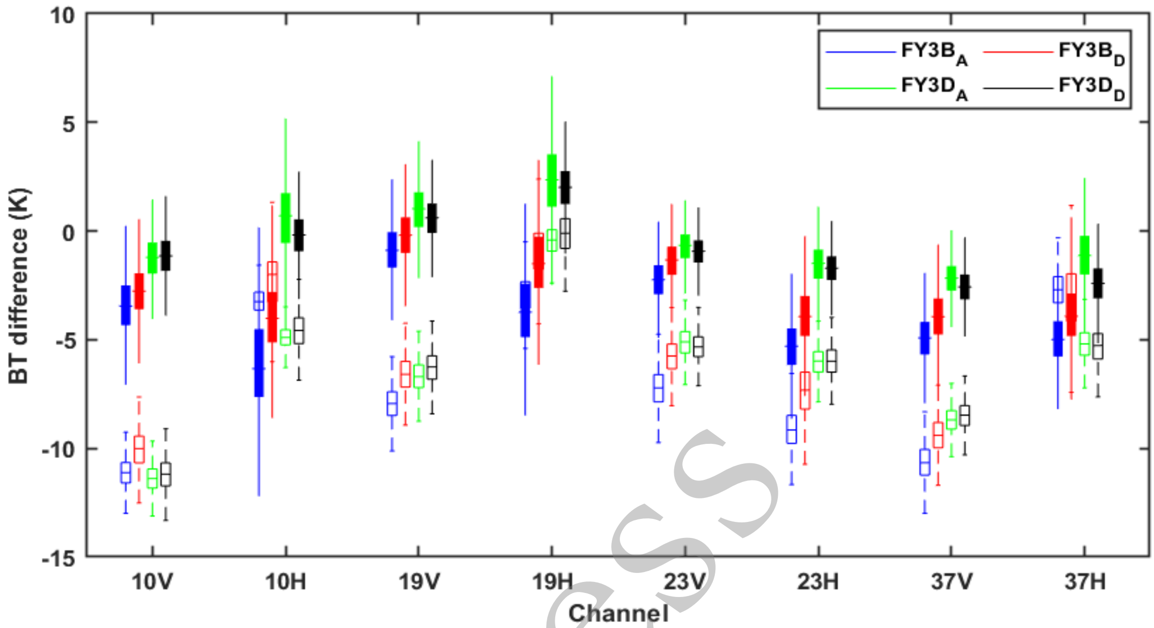

Fig.4 The boxplot of BT difference between MWRI and AMSR2 for the ascending and descending orbits of MWRI/FY3B (2012-2019) and MWRI/FY3D (2018-2019) over land (filled) and water (unfilled).

4. Discussions of the BT difference between MWRI and AMSR2

In the above comparisons, substantial BT differences between MWRI and AMSR2 were found over water. The potential causes for this difference are explored here by using the simultaneous conical overpassing (SCO) method and RTM simulations.

4.1. SCO method

To inter-calibrate radiometers on different polar-orbiting satellites to achieve consistency and traceability, the SCO method was widely used to calibrate conically scanning instruments and to remove biases, such as SSMIS and SSMI (Yan and Weng, 2008;

Weng et al. 2009). The SCO method is adopted from the Simultaneous Nadir Overpasses (SNO) technique developed by Cao et al (2004). The SNO method has been used for the construction of long-term records of the Microwave Sounding Unit (MSU) and the Advanced Microwave Sounding Unit-A (AMSU-A) (Zou et al., 2006; Iacovazzi and Cao, 2007).

Considering MWRI and AMSR2 are conically scanning and have more chance of matching with closer ETC, the SCO method was used to explore the BT difference between AMSR2 and MWRI/FY3D during July 1-3, 2018. To obtain more matching in high latitudes where surface and atmosphere are relatively stable, the SCO constraint on the distance window from two sensors is set to a ground distance of 5 km, and the time window is set to 60 s although SNO (or SCO) events occurring within a few seconds for succeeding satellites.

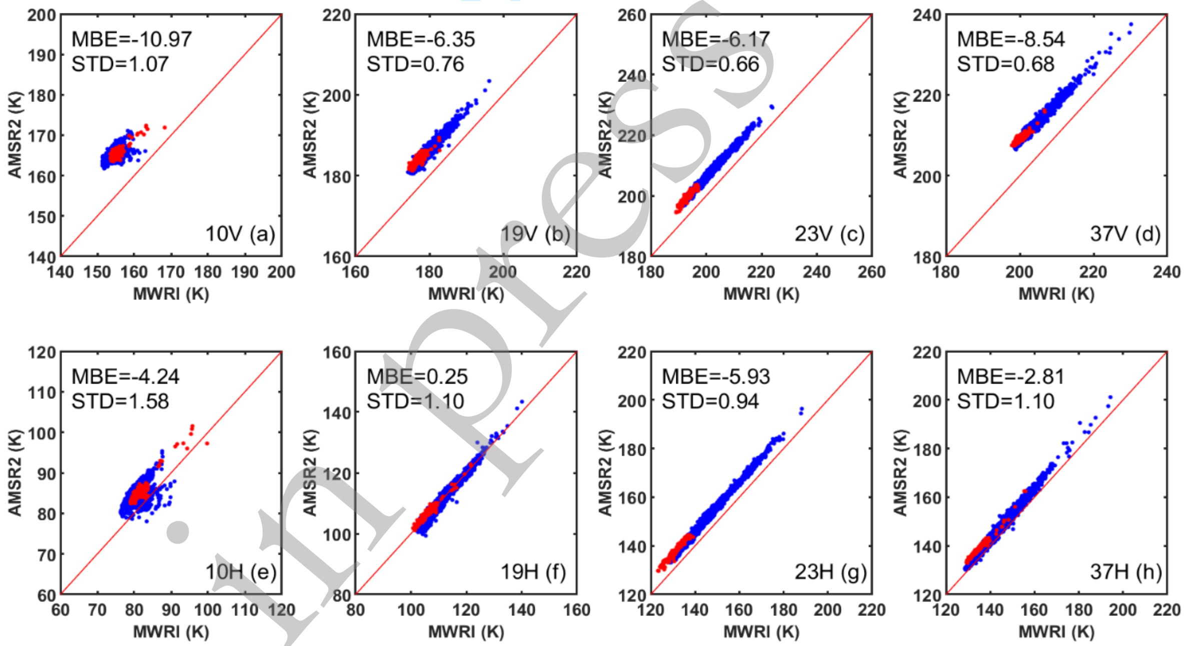

Fig.5 Scattering plots of the SCO pairs between MWRI/FY3D and AMSR2 at 8 channels over water, and the colors stand for the pairs located in the north-polar (blue) and south-polar (red) regions.

The SCO pairs of MWRI and AMSR2 over water mostly occurred from the latitude around ±75° on July 1, 2018. Both BT for SCO pairs are compared in Fig.5, where colors are used to distinguish samples located in the north polar (blue) and south polar (red) regions. It is also found in Fig.5 that BT differences of MWRI and AMSR2 at 10V and 37V are more significant, and the MBE at the 8 channels are close to those obtained in the previous section, although the matching number (~3200) is far less than that, which imply that these BT differences are relatively stable and independent of the selected region.

4.2. Using RTM simulations as reference

RTM is a bridge that connects observations and theoretical radiation, which has been widely used for satellite observation cross-validations (Clought et al, 2004; Goldberg et al.,2001; Lu et al., 2011). Hence, we combined the atmospheric profiles derived from reanalysis data ERA5 (1hr/0.25°) with a fast microwave radiative transfer model, MWRT (Liu, 1998), to obtain the BT simulations for AMSR2 in 55° and MWRI in 53.1° incident angle, respectively. Firstly, both BT observations over land were compared with the corresponding model simulations, which shows a slight change (<0.1K) in BT simulations at different incident angles. Then, we focused on the substantial BT difference of MWRI-AMSR2 pairs in the vertical polarization channels over water.

Fig.6 shows the scattering plots between both BT simulations and the corresponding MWRI-AMSR2 observations at the vertically polarized channels over water. To see the influence of incident angle on simulations clearly, BT simulations for AMSR2 (blue) and MWRI (red) are plotted in a panel for the same channel. Noted that we only selected ERA5 data at 05hr (UTC) on July 1, 2018, to do the simulation testing, so the available matched samples are limited (~790). First, it is seen in Fig.6(a-d) that the simulated AMSR2 BTs (blue) at the four vertical channels are more consistent with the corresponding AMSR2 observations (with the MBE less than 0.5 K and STD less than 1.3 K), which demonstrates that the AMSR2 BT simulations are reasonable and reliable. In the comparisons of AMSR2 observations with MWRI BT simulations (red), AMSR2 observations are higher than 2- 4 K due to the 2° incident angle difference. Second, MWRI observations and both simulations are compared at four vertical polarization channels (Fig.6(e-h)) and show that MWRI observations are generally lower than its BT simulations (red), especially about 6 K lower at

10V and 37V. The corresponding BT difference between MWRI observations and AMSR2 simulations (blue) in Fig.6(e-h) is close to the results derived from both BT observations.

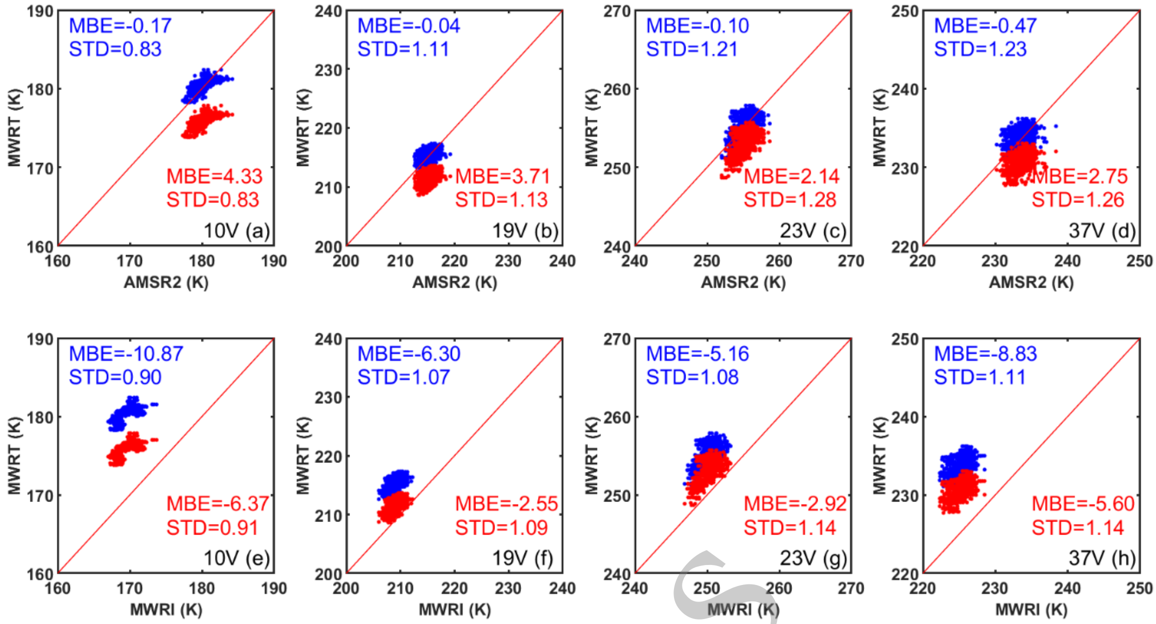

Fig.6 BT difference between MWRI-AMSR2 BT observations and the corresponding BT simulations (MWRT for short) for AMSR2 (blue,55°) and MWRI (red,53.1°) at the vertically polarized channels, and the corresponding statistics parameters are shown with the same color.

Therefore, using model simulations as a reference, we can see that the significant BT difference at the vertically polarized channels over water is mainly due to the different incident angles and the underestimated MWRI BT observations. To better understand the effect of both, the contribution of each to the total BT difference was calculated and shown in Fig.7. For the four vertically polarized channels, the lower MWRI observation accounts for 60% of the total difference at 10V and 37V, and the incident angle accounts for 40%; while both proportions are reversed at 19V. As to 23V, the contribution of both sides is almost equal, each accounting for 50%.

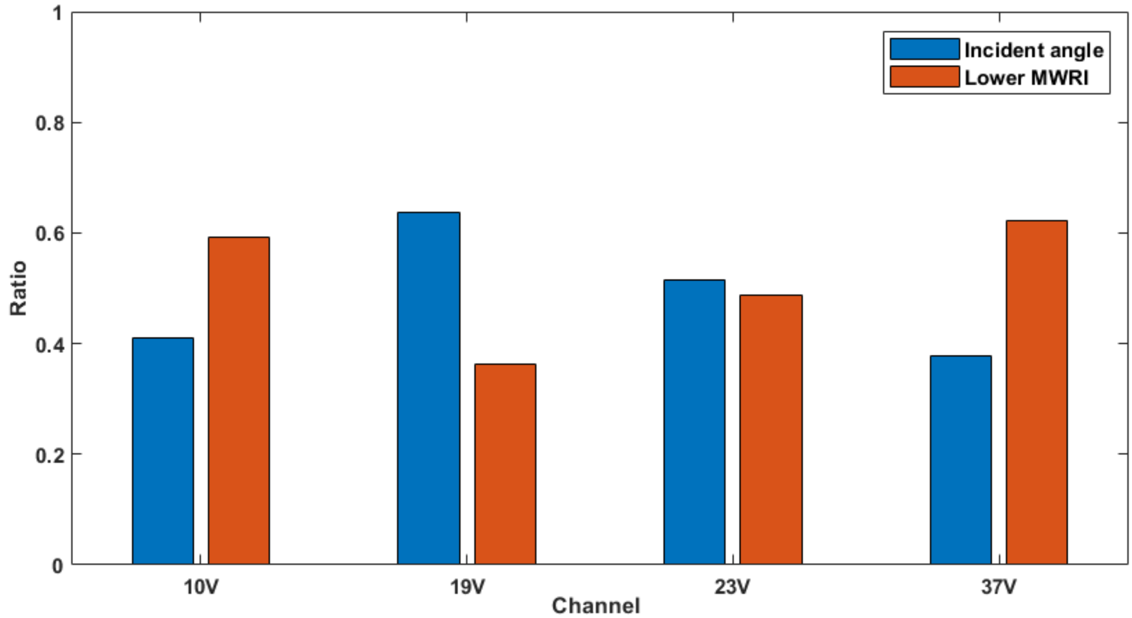

Fig.7 Ratio of the contribution of incident angle and lower MWRI to MWRI-AMSR2 total BT difference

5. Preliminary assessment of the recalibrated MWRI BT

The MWRI BT we used above is the operational calibrated data. To check the quality of MWRI BT more, the recalibrated MWRI BT (DOI: 10.12185/NSMC.RICHCEOS.FCDR.MWRIRecalOrb.FY3.MWRI.L1.GBAL.POAD. NUL. 010KM. HDF.2021.2.V1, Wu et al. (2010)) were used to demonstrate the necessary and valid of recalibrations. The recalibrated MWRI BT is developed by the Laboratory of Radiometric Calibration and Validation for Environmental Satellites, National Satellite Meteorological Center, China Meteorological Administration. This dataset is based on the original level-0 MWRI data on the FY-3 series satellites and adopts the new and improved calibration algorithm based on MWRI operational calibration algorithm. The main algorithm improvements include the radiation correction of the microwave imager's hot mirror back lobe, the hot mirror emissivity correction, the heat source efficiency correction, and the receiver nonlinear correction.

Here we chose the same period recalibrated MWRI BT on FY3B and FY3D from 2012 to 2019, then used the same treatments to match with AMSR2 observations and model simulations as mentioned above. We still focus on the matching pairs over the water surface due to the obvious BT difference as mentioned above. To see the difference, the matched AMSR2 and both MWRI BT (the operational calibration (blue) and the recalibration(red)) are plotted in a panel as Fig.8 shown. It is seen that the MBE of AMSR2-MWRI for the recalibrated one is obviously reduced at the vertically polarized channels, especially at 10V and 37V the difference is significantly reduced by more than 50%. Relatively, the changes at 18.7 GHz and 23.8 GHz are small with a high overlap between the operational and recalibrated data.

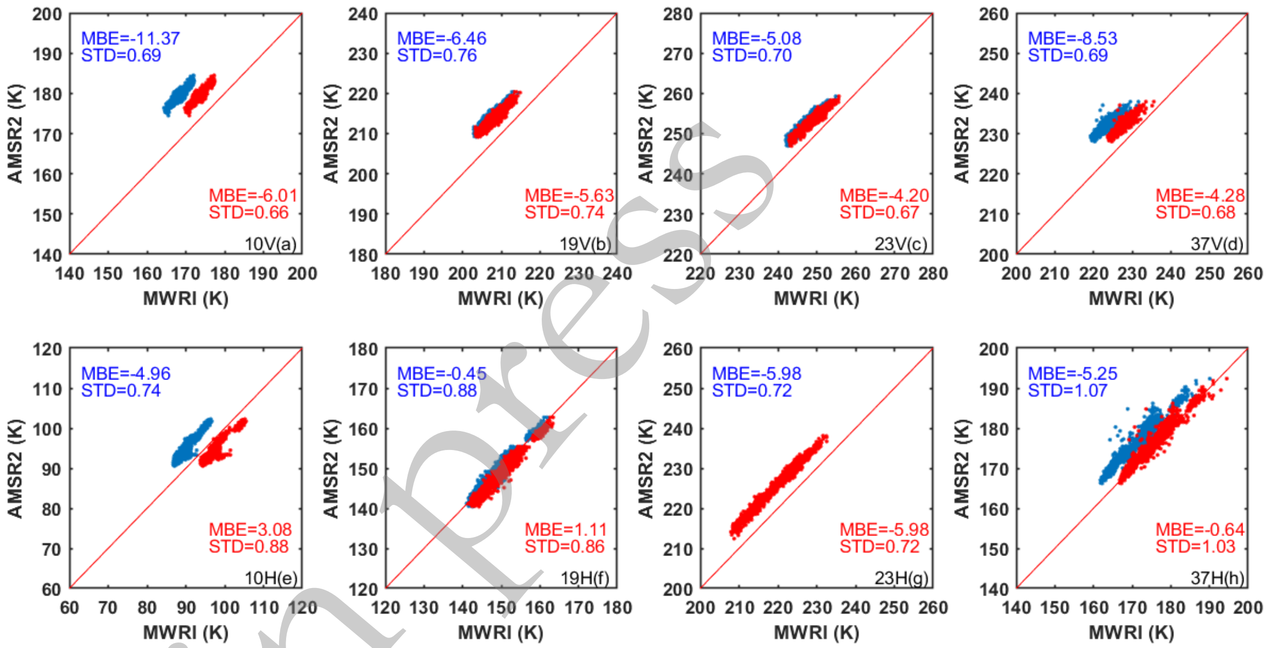

Fig.8 Scatter plots of matched BT at 8 channels for AMSR2-MWRI/FY3D in 2018-2019 over water, and the colors stand for the operational (blue) and recalibrated(red) MWRI BT. The corresponding statistics parameters are shown in the same color.

To better understand the long-term performance of the recalibrated MWRI BT data, the annual BT difference between AMSR2 and recalibrated MWRI/FY3B during 2012-2019 is shown in Fig.9. Compared with the operational calibrated MWRI results in Fig.3, it is clearly seen that over land the annual median BT differences at most of channels are close to zero, and has little change in eight years. Over water, the annual median BT differences at the vertical polarization channels are significantly reduced to 5 K and more constant in eight years. These reduced and more stable BT differences on both land and water demonstrate the improvement of the recalibrated MWRI BTs, except for 23H, where the BT differences on land and water are still large.

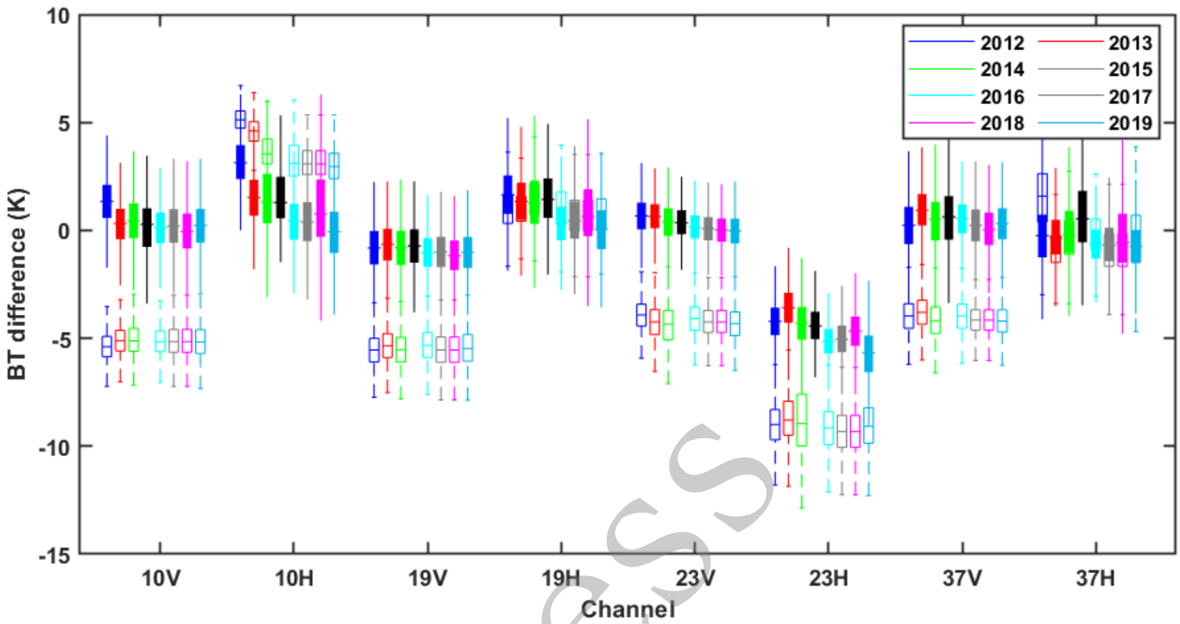

Fig.9 Same as Fig.3 except for the recalibrated MWRI BT

Then using model results in 4.2 as media reference, the relationships between AMSR2 and the recalibrated MWRI BT observations are shown in Fig.10. Firstly, AMSR2 results in Fig.10 (a-d) are quite close to those shown in Fig.6(a-d), that is, AMSR2 observations are higher MWRI more than 2-4 K due to 2° incident angle difference. However, the recalibrated MWRI BT results in Fig.10 (e-h) show significant improvements, for example, the MWRI observations are closer to their BT simulations (red), especially at 10V and 37V, whose MBE is reduced from 5-6 K in Fig.6 (e-h) to 1.5 K, suggesting that the recalibrated MWRI BT has removed the underestimated effect at 10V and 37V of the operational MWRI BT over water. Relatively, the updated effect on 18V and 23V is weak, about 0.5 K. Additional, the BT difference of MWRI observations and AMSR2 simulations (blue) in Fig.10 (e-h) also reflects the reduced BT difference, compared to the corresponding results in Fig.6 (e-h), particularly at 10V and 37V, because the obvious underestimation in the operational data has been corrected, and only remain the BT difference caused by the 2° incident angle difference.

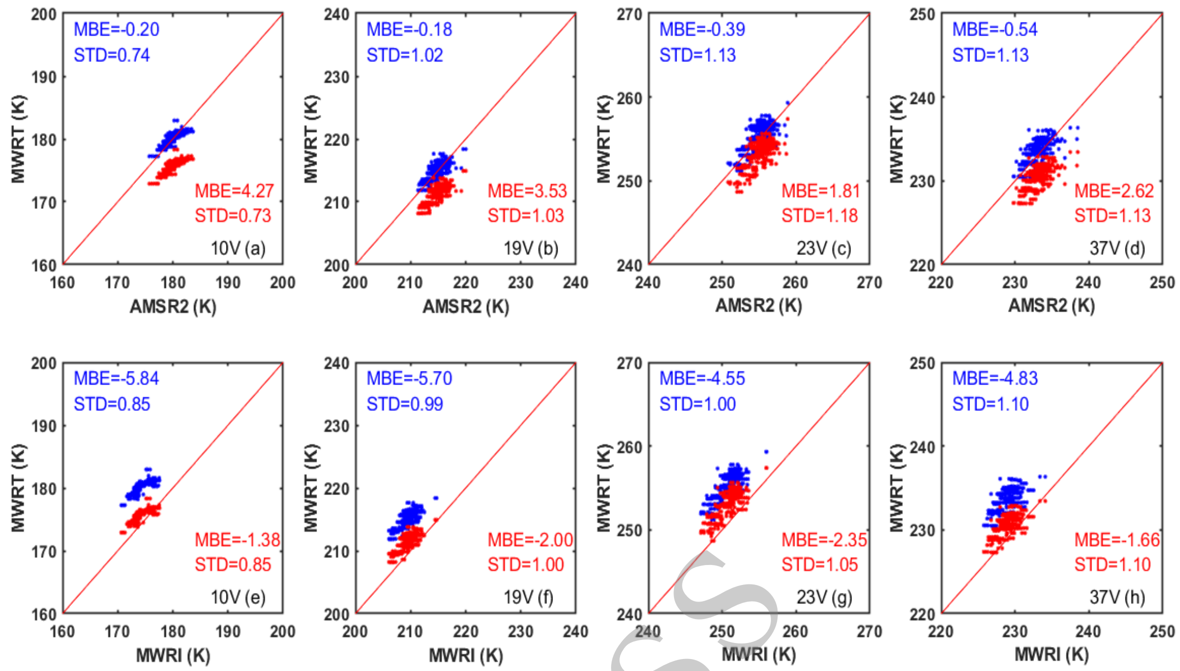

Fig.10 Same as Fig.6 except for the recalibrated MWRI BT

6. Conclusions

MWRIs on FY-3 serial satellites have been launched, providing rich data for monitoring cloud, precipitation and ground. To better understand the long-term performance of MWRI, we carefully compared the operational MWRI BT on FY-3B/3D and AMSR2 on GCOM-W1 from 2013 to 2019. The comparisons were made over land and water. The SCO method and RTM simulations were also used in the comparison, as well as the preliminary assessment of recalibrated MWRI data. Major conclusions are as follows.

1) On both FY-3B and FY-3D satellites, the majority of MWRI BTs were smaller than AMSR2 measurements, especially at the vertical polarization channels over water, most MBEs exceed 5 K, even up to 10 K at 10V and 37V.

2) Overland, the BT difference was reduced from 2-4 K on FY3B to about 0-2 K on FY3D, and the ascending and descending orbit difference for MWRI/FY3D is much smaller than that for MWRI/FY3B, reflecting the improvement of MWRI onboard FY3D.

3) The operational MWRI BTs have significantly correlated with those of AMSR2 and BT difference for MWRI/FY3B during 2012-2019 was gradual enhanced over time and more stable for MWRI/FY3D in 2018-209.

4) Similar BT difference was found over polar water by using the SCO method, which implied that these BT differences were more stable and independent of the selected region.

5) Substantial BT differences at the vertical polarization channels of MWRI-AMSR2 over water were partly due to the different incident angles; however, the underestimation of the operational MWRI BT over the water was still a very important issue.

6) The recalibrated MWRI BT can significantly improve the quality of the operational MWRI BT observations at the vertical polarization channels, especially effectively removing the underestimation at 10V and 37V over water.

It is important to note that the current conclusions are obtained based on limited observations (e.g., randomly selected dates, the first 5 days in July) in 2012-2019 over China and the polar region. We also need to examine the seasonal and spatial variation of BT differences and explore their causes using more MWRI and AMSR2 observations, and other references, and consider the effect of cloud presence on observed pixels to better understand MWRI observation quality on FY-3 series satellites.

Acknowledgments. This work is supported by the National Natural Science Foundation of China (Grant number 41575033) and the National Key R&D Program of China (Grant number 2017YFC1501700). Thanks to the China Meteorological Administration-National Satellite Weather Center for MWRI data support. Thanks to the NASA GES DISC for the L1C AMSR2 data support. Thanks to ECMWF for ERA5(hourly and 0.25°) data support. Thanks to Prof. Liu Guosheng working at Florida State University for MWRT model support.

REFERENCES

Berg, W., S. Bilanow, R. Chen, *et al.*, 2016: Intercalibration of the GPM Microwave Radiometer Constellation. *J. Atmos. Ocean. Technol.*, 33, 2639–2654.

Cao, C., M. Weinreb, and H. Xu, 2004: Predicting simultaneous nadir overpasses among polar-orbiting meteorological satellites for the intersatellite calibration of radiometers. *J. Atmos. Oceanic Technol.*, 21, 537–542.

Chen, B. Y., S. Y. Gu, F. S. Chen, 2016: Super resolution image reconstruction for FY-3 MWRI 10.6 GHz band. *Journal of Applied Meteorology*, 27(1), 123-128, Doi:1011898/1001-7313.20160113. (in Chinese)

Clough, S.A., M. W. Shephard, E. J., Mlawer, *et al.*, 2005: Atmospheric radiative transfer modeling: A summary of the AER codes. *Journal of Quantitative Spectroscopy and Radiative Transfer,* 91,233-244. doi:10.1016/j.jqsrt.2004.05.058.

Chen, W. Y., G. F. Liu, J. He, *et al.*, 2019: Research on the method of reducing the receiver non-linear deviation of the Microwave Radiation Image. *Remote sensing technology and application*, 32(1), 121-125. (in Chinese)

Cui, Y. K., D. Long, Y. Hong, C. Zeng, J. Zhou, Z. Y. Han, R. H. Liu, W. Wan, 2016: Validation and reconstruction of FY-3B/MWRI soil moisture using an artificial neural network based on reconstructed MODIS optical products over the Tibetan Plateau. *Journal of Hydrology*, 543, 242-254.

Dong, C. H., J. Yang, Z. D. Yang, *et al.*, 2009: An overview of a new Chinese weather satellite FY-3A. *Bull Amer Meteor Soc,* 90, 1531-1544.

Dong, K. S.， X. X. Xie， X. Li and W. L. Liu, 2020: Nonlinear characteristics of FY-3D microwave radiation imager and an optimal calculation method. *Journal of Remote Sensing*, 24(3), 226-232, DOI：10.11834/jrs.20208274. (in Chinese)

Ebuchi1 Naoto, M. Kachi, M. Kasahara, H. Fujii, R. Shimada, K. Ohara, T. Maeda, K. Inaoka, Y. Kojima, 2021: Present Status of AMSR2 on GCOM-W and AMSR3 on GOSAT-GW. The 2021 International Ocean Vector Winds Science Team meeting, https://mdc.coaps.fsu.edu/scatterometry/meeting/docs/2021/Ebuchi_IOVWST2020_rev2.pdf.

Goldberg, M. D.; Crosby, D. S.; Zhou, L.H., 2001: The limb adjustment of AMSU-A observations: Methodology and validation. *J. Appl. Meteor.* 2001, 40, 70-83.

doi:10.1175/1520-0450(2001).

Gu S. Y., Y. Guo, F. Dou, *et al*., 2021: Radiometric Calibration Technology of Microwave Atmospheric Sounders of FY-3 Satellites. *Remote Sensing Technology and Application*, 36(1):141-154. (in Chinese)

Houz, A. Y., R. K. Kakar, S. Neeck, A. A. Azarbarzin, C. D. Kummerow, M. Kojima, R. Oki, K. Nakamura, and T. Iguchi, 2014: The Global Precipitation Measurement mission. *Bull. Amer. Soc.*, 95, 701-722, doi:10.1175/BAMS-D-13-00164.1

Iacovazzi R. and C. Cao, 2007: Reducing uncertainties of SNO-estimated intersatellite AMSU-A brightness temperature biases for surface-sensitive channels. *J. Atmos. Oceanic Tech.*, 25, 1048 – 1054.

Lawrence, H., F. Carminati, W. Bell, *et al*., 2017: An evaluation of FY-3C MWRI and Assessment of the long-term quality of FY-3C MWHS-2 at ECMWF and the Met Office. ECMWF Technical Memoranda, 798.

Li, R., and Coauthors, 2022: Spatiotemporal variations of Microwave Land Surface Emissivity (MLSE) over China derived from four-year recalibrated Fengyun 3B MWRI data. Adv. Atmos. Sci., 39(9), 1536−1560, https://doi.org/10.1007/s00376-022-1314-0.

Liu, G. F., S. Wu, W. Y. Chen, 2014: Calibration system and achievement of Microwave Radiation Imager of FY-3 satellite. *Journal of Microwave*, 576-579. (in Chinese).

Liu, G. S., 1998: A fast and accurate model for microwave radiance calculations. J. Meteor. Soc. Japan, 76(2), 335−343, https://doi.org/10.2151/JMSJ1965.76.2_335.

Liu, J. Z., W. F. Li, J. T. Peng, L. J. Shen, H. Han, P. Zhang, and L. Yang, 2021: Geolocation error estimation and correction on long-term MWRI data. IEEE Trans. Geosci. Remote Sens., 59, 9448−9461, https://doi.org/10.1109/TGRS.2021. 3051199.

Lu, N. M., and S.Y. Gu, 2016: Review and prospect on the development of meteorological satellites. *Journal of Remote Sensing*, 20(5), 832-841. (in Chinese)

Lu, Q. F.; Bell, W.; Bauer, P.; Bormann, N.; Peubey, C.,2011: An evaluation of FY-3A satellite data for numerical weather prediction. *Quart. J. Roy. Meteor. Soc.* 2011,137, 1298-1311, doi:10.1002/qj.834.

Qiao, M., H. Yang, J. K. He and L. Q. Lv, 2012: On-orbit performance stability analysis of microwave radiometer imager onboard FY-3 Satellite. *Journal of Remote Sensing*, 16(6), 1246-1261. (in Chinese)

Skofronick-Jackson, G., W.A. Petersen, W.Berg, et al., 2017: The Global Precipitation Measurement (GPM) Mission for Science and Society. *Bull. Am. Meteorol. Soc.,* 98, 1679–1695.

Song, H., G. Wang, A. Cao, *et al.*, 2017: Improving the spatial resolution of FY-3 Microwave Radiation Imager via fusion with FY-3/MERSI. *IEEE Journal of Selected Topics in Applied Earth Observations and Remote Sensing*, 10, 3055-3063, DOI: 10.1109/JSTARS.2017.2665524.

Takashi, M., Y. Taniguchi, K. Imaoka, 2015: GCOM-W1 AMSR2 Level 1R product: dataset of brightness temperature modified using the antenna pattern matching technique. *IEEE Transactions on Geoscience and Remote Sensing*, 54, 1-13.

Tang, F., H. J. Dong, N. Li, C. H. Liu, 2016: Geolocation errors and correction of FY-3B microwave radiation imager measurements. *Journal of Remote Sensing*, 20(6), 1342-1351, DOI: 10.11834/jrs.20165279. (in Chinese)

Tang, F., X. Zou, 2017: Liquid water path retrieval using the lowest frequency channels of *Fengyun-3C* Microwave Radiation Imager (MWRI). *J Meteorol Res*, 31, 1109-1122.

Weng, F., S. Yang, N. Sun, and B. Yan, 2009: SSM/I intersensor calibration produces improved climate trends. GSICS Quart., 3, 2-3.

Wentz, F. J. and D. Draper, 2016: On-orbit absolute calibration of the Global Precipitation Measurement Microwave Imager. *J. Atmos. Oceanic Technol.*, 33, 1393–1412, doi:10.1175/JTECH-D-15-0212.1.

Wu Shengli, Sun Ling, Lu Qifeng, Xu Hongxin, He Jiakai, Sun Fenglin, Gu Songyan, Zhang Peng. FY-3B/C/D Microwave Imager Recalibration Orbit Dataset. National Satellite Meteorological Center. [2010.doi:10.12185/NSMC.RICHCEOS.FCDR.MWRIRecal Orb. FY3.MWRI.L1.GBAL.POAD.NUL.010KM.HDF.2021.2.V1]

Xian, D., P. Zhang, L. Gao, R. J. Sun, H. Z. Zhang, and X. Jia, 2021: Fengyun meteorological satellite products for earth system science applications. Adv. Atmos. Sci., 38(8), 1267−1284, https://doi.org/10.1007/s00376-021-0425-3.

Yan B., F. Weng, 2008: Intercalibration between Special Sensor Microwave Imager/Sounder and Special Sensor Microwave Imager. *IEEE Trans. Geosci. Remote Sens.*, 46, 984–995.

Yang, H., L. Lv, N. M. Lu, G. Liu, M. Bai, Q. Qian, J. He, and H. Xu, 2011: The Feng-Yun-3 microwave radiation imager on-orbit verification. *IEEE Trans. Geoscience. Rem. Sensing.*, 49,4552-4560.

Yang, J., C. H. Dong, N. M. Lu, et al., 2009: FY-3A: the New Generation Polar-Orbiting Meteorological Satellite of China. *Acta Meteorologica Sinica*, 67(4), 501-509.

Zeng Z, G. Jiang, 2021: Intercalibration of the Microwave Radiation Imager on Fengyun 3C. *Remote Sensing Technology and Application*，36(3):682-691. (in Chinese)

Zhang, M., H. Qiu, X. Fang, N. M. Lu, 2015: Study on multivariate statistical estimation method of tropical cyclone intensity based on FengYun-3 Microwave Imager. *Journal of tropical meteorology*, 31(1), 87-94. (in Chinese)

Zhang, M., Q. F. Lu, S. Y. Gu, X. Q. Hu, S. L. Wu, 2019: Analysis and correction of the difference between the ascending and descending orbits of the FY-3C microwave imager. *Journal of Remote Sensing*, 23(5), 841-849, DOI:10.11834/jrs.20198235. (in Chinese)

Zhang, P., and Coauthors, 2019: Latest progress of the Chinese meteorological satellite program and core data processing technologies. Adv. Atmos. Sci., 36, 1027−1045, https://doi.org/10.1007/s00376-019-8215-x.

Zhang, P., X. Q. Hu, Q. F. Lu, A. J. Zhu, M. Y. Lin, L. Sun, L. Chen, and N. Xu, 2022: FY-3E: The first operational meteorological satellite mission in an early morning orbit. Adv. Atmos. Sci., 39(1), 1−8, https://doi.org/10.1007/s00376-021-1304-7.

Zou, C.Z., M. D. Goldberg, Z. Cheng, N. C. Grody, J. T. Sullivan, C. Cao, and D. Tarpley, 2006: Recalibration of microwave sounding unit for climate studies using simultaneous nadir overpasses. *J. Geophys. Res.,* 111, D19114, doi:10.1029/2005JD006798.